a few ions of geochemical interest. In dilute solution, diffusion coefficients depend approximately on the square root of ionic strength. In more concentrated solutions, diffusion coefficients show a complex dependence on ionic strength, the treatment of which is beyond the scope of this book. Discussions of this problem may be found in Anderson (1981), Tyrell and Harris (1984), and Lasaga (1997).

5.5 SURFACES, INTERFACES, AND INTERFACE PROCESSES

The properties of a phase at its surface are different from the bulk properties of the phase. This difference arises from the difference between the local environment of atoms on a surface or interface and those in the interior of a phase. An atom at the surface of a crystal is not surrounded by the same bonds and distribution of charges as it would be in the interior of the crystal lattice. Its potential energy must therefore be different. Here we define *surface* as the exterior boundary of a condensed phase (a solid or liquid) in a vacuum or gas. An *interface* is the boundary between two condensed phases, for example, between two crystals or between a mineral and water (the term "surface" is, however, often used for what we have just defined as an interface). Surfaces, surface energies, and interfaces play an important role in many geochemical processes. All heterogeneous reactions (i.e., those involving more than one phase) must involve interfaces or surfaces. Dissolution, melting, exsolution, and precipitation are examples of processes that, on an atomic scale, occur entirely at or near the interface between two phases. Surfaces can also play important roles as catalysts in many geochemical reactions.

On a microscopic scale, the reactivity of mineral surfaces will vary locally for several reasons. The first is the microtopography of the surface (Figure 5.21). For example, a single growth unit (which might be a single atom, an ion, or molecule and called an *adatom*), located on an otherwise flat surface will be particularly unstable because it is bonded to other units on only one side. A *step* (which might be formed through growth, dissolution, or *screw dislocation*) provides a more favorable growth site because the new unit is bound to other units on two sides. An even better site for growth is at a *kink*, where bonds may be formed on three sides. Conversely, a unit at a kink (with three exposed sides) is less stable than one at a step (with two exposed sides), which in turn is less stable than a unit on a flat surface, with only one exposed side. The point is, kinks and steps will be more reactive than other features, so surface reactions rates will depend in part on the density of these features.

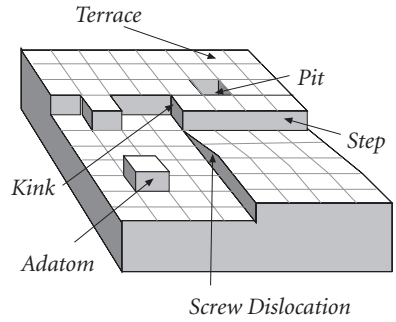

Figure 5.21 On a microscopic scale, the surface of a mineral exhibits a number of features. As a result, the local reactivity of the surface will be quite variable.

Properties of mineral surfaces will also vary depending on the orientation of the surface relative to crystallographic axes. Most minerals grow or dissolve faster in one direction than in another. Most surface reactions involve the formation of new bonds between atoms of a mineral and atoms of the adjacent phase; the nature of the bonds that are possible will depend on the orientation of the surface relative to crystallographic axes. Reaction rates measured for one crystal face may not be representative of other faces.

Finally, almost all minerals have a variety of atoms and crystallographic sites, hence there will be a variety of bonds that are possible on any surface. We will discuss this aspect of surfaces in slightly more detail below.

5.5.1 The surface free energy

In Chapters 2 and 3, we introduced the concept of molar quantities and partial molar quantities. For example, the molar volume of a substance was:

$$\bar{V} = \frac{V}{n}$$

and we defined the partial molar volume as:

$$v_i^{\phi} = \left(\frac{\partial V}{\partial n_i}\right)_{T,P,n_j} \qquad (3.11)$$

We now define two new quantities, the *molar surface area*:

$$\bar{A} = \frac{A}{n} \qquad (5.105)$$

and the *partial molar surface area*:

$$a_i^{\phi} = \left(\frac{\partial A}{\partial n_i}\right)_{T,P,n_j} \qquad (5.106)$$

where A is the surface area of the phase and n is the number of moles of the component. The molar volume or the molar Gibbs free energy of pure quartz depends only on temperature and pressure. Thus the molar volume of each (pure) quartz crystal is the same as that of every other (pure) quartz crystal at that temperature and pressure. Unlike other molar quantities, the *molar surface area and partial molar surface area depend on shape and size*, and are therefore not intrinsic properties of the substance. For a sphere, for example, the partial molar surface area is related to molar volume as:

$$a = \frac{\partial A}{\partial V}\frac{\partial V}{\partial n} = \frac{2v}{r} \qquad (5.107)$$

For other shapes, the relationship between a and v will be different.

Finally, we define the *surface free energy* of phase ϕ as:

$$\sigma^{\phi} \equiv \left(\frac{\partial G}{\partial A}\right)^{\phi}_{T,P,n} \qquad (5.108)$$

The surface free energy represents those energetic effects that arise because of the difference in atomic environment on the surface of a phase. Surface free energy is closely related to surface tension. The total surface free energy of a phase is minimized by minimizing the phase's surface area. Thus a water-drop in the absence of other forces will tend to form a sphere, the shape that minimizes surface area. When surface effects must be considered we can revise the Gibbs free energy equation (eqn. 3.14) to be:

$$dG = VdP - SdT + \sum_i \mu_i dn_i + \sum_k \sigma_k dA_k \qquad (5.109)$$

where the last sum is taken over all the interfaces of a system. In this sense different crystallographic faces have different surface free energies. The last term in eqn. 5.109 increases in importance as size decreases. This is because the surface area for a given volume or mass of a phase will be greatest when particle size is small.

5.5.2 The Kelvin effect

When the size of phases involved is sufficiently small, surface free energy can have the effect of displacing equilibrium. For an equilibrium system at constant temperature and pressure, eqn. 5.109 becomes:

$$0 = \sum_i \nu_i \mu_i^o + RT\sum_i \nu_i \ln a_i + \sum_k \sigma_k dA_k$$

The first term on the right is $\Delta G°$, which according to eqn. 3.86 is equal to $-RT \ln K$. This is the "normal" equilibrium constant, uninfluenced by surface free energy, so we'll call it K°. We will call the summation in the second term K^s, the equilibrium influenced by surface free energy. Making these substitutions and rearranging, we have:

$$\ln K^s = \ln K° - \frac{\sum \sigma_k dA_k}{RT} \qquad (5.110)$$

Thus we predict that equilibrium can be shifted due to surface free energy, and the shift will depend on the surface or interfacial area. This is known as the *Kelvin effect*.

There are a number of examples of this effect. For example, fine, and therefore high surface area, particles are more soluble than coarser particles of the same composition. Water has a surface free energy of about 70 mJ/m^2. Consequently, humidity in clouds and fogs can reach 110% when droplet size is small.

5.5.3 Nucleation and crystal growth

5.5.3.1 Nucleation

Liquids often become significantly oversaturated with respect to some species before crystallization begins. This applies to silicate liquids as well as aqueous solutions (surface seawater is several times oversaturated with respect to calcite). However, crystallization of such supersaturated solutions will often begin as soon as seed crystals are added. This suggests that nucleation is an important barrier to crystallization. This barrier arises because the formation of a crystal requires a local increase in free energy due to the surface free energy at the solid–liquid interface.

Let's explore a bit further how nucleation can be inhibited. For a crystal growing in a liquid, we can express the complete free energy change as:

$$dG_{tot} = \sigma dA + dG_{xt} \qquad (5.111)$$

where dG_{xt} refers to the free energy change of the crystallization reaction that applies throughout the volume of the crystal (i.e., free energy in the usual sense, neglecting surface effects).

Let's consider a more specific example, that of a spherical crystal of phase ϕ growing from a liquid solution of component ϕ. The free energy change over some finite growth interval is:

$$\Delta G_{tot} = 4\pi r^2\sigma + \frac{4}{3}\pi r^3 \frac{\Delta G_{xt}}{\bar{V}} \qquad (5.112)$$

where r is the radius (we divide by $\bar{V}$ to convert joules per mole to joules per unit volume). The first term on the right is the surface free energy, and, although small, *is always positive*. At the point where the solution is exactly saturated, ΔG will be 0. The net free energy, ΔG_{tot}, is thus positive, so the crystal will tend to dissolve. In order for spontaneous nucleation to occur, the second term on the right must be negative and its absolute value must exceed that of the first term on the right of 5.112 (i.e., the liquid must be supersaturated for nucleation to occur). Solving eqn. 5.112 for r, we find $\Delta G_{tot} \leq 0$ when $r \geq -3\sigma/\Delta G$.

How will ΔG vary with r up to this point? To answer this, we differentiate eqn. 5.112 with respect to r:

$$\frac{\partial \Delta G_{tot}}{\partial r} = 8\pi r\sigma + 4\pi r^2 \frac{\Delta G_{xt}}{\bar{V}} \qquad (5.113)$$

Since the volume free energy term is proportional to r^2 and the surface free energy term to r, the latter necessarily dominates at very small values of r. For small values of r, ΔG_{tot} will increase with increasing r because σ is always positive. In other words, near the saturation point where ΔG is small, very small crystals will become increasingly unstable as they grow. The critical value of r, that is, the value at which ΔG will decrease upon further growth, occurs where $\partial G/\partial r = 0$. Solving eqn. 5.113, we find that

$$r_{crit} = -\frac{2\sigma}{\Delta G_{xt} / \bar{V}} \qquad (5.114)$$

For a solution that undergoes cooling and becomes increasingly saturated as a result (e.g., a magma or a cooling hydrothermal solution), we can use eqn. 5.68 to approximate the ΔG term (i.e., $\Delta G \cong -\Delta T\Delta S$, where ΔT is the difference between actual temperature and the temperature at which saturation occurs, and ΔS is the entropy change of crystallization). Figure 5.22 shows the total free energy calculated in this way as a function of r for various amounts of undercooling.

The surface free energy term correlates with viscosity. Thus nucleation should require less supersaturation for aqueous solutions

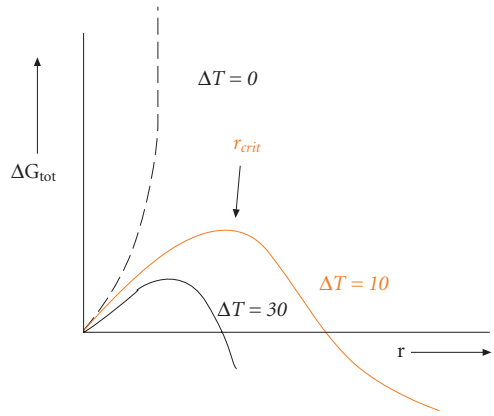

Figure 5.22 Free energy as a function of crystal radius for small crystals forming near the saturation point. ΔT is the amount of undercooling (difference between temperature and saturation temperature).

than silicate melts. Among silicate melts, nucleation should occur more readily in basaltic ones, which have low viscosities, than in rhyolitic ones, which have high viscosities. This is what one observes. Also, we might expect rapid cooling to lead to greater supersaturation than slow cooling. This is because there is an element of chance involved in formation of a crystal nucleus (the chance of bringing enough of the necessary components together in the liquid so that r exceeds r_{crit}). Slow cooling provides time for this statistically unlikely event to occur, and prevents high degrees of supersaturation from arising. With rapid cooling, crystallization is postponed until ΔG_r is large, when many nuclei will be produced. Let's briefly consider nucleation rates in more detail.

5.5.3.2 Nucleation rate

The first step in crystallization from a liquid is the formation of small clusters of atoms having the composition of the crystallizing phase. These so-called *heterophase fluctuations* arise purely because of statistical fluctuations in the distribution of atoms and molecules in the liquid. These fluctuations cause local variations in the free energy of the liquid, and therefore their distribution can be described by the Boltzmann distribution law:

$$N_i = N_v e^{-\Delta G_{xt}/\mathrm{k}T}$$

where N_i is the number of clusters per unit volume containing i atoms, N_v is the number of atoms per unit volume of the cluster, and ΔG_i is the difference between the free energy of the cluster and that of the liquid as a whole. The number of clusters having the critical size (r_{crit}) is:

$$N_{crit} = N_v e^{-\Delta G_{crit}/\mathrm{k}T}$$

where ΔG_{crit} is the total free energy (ΔG_{tot}) of clusters with critical radius obtained by solving eqn. 5.111 when $r = r_{crit}$. For spherical clusters, this is:

$$\Delta G_{crit} = \frac{16\pi}{3}\frac{\sigma^3 \bar{V}}{\Delta G_{xt}^2} \qquad (5.115)$$

Substituting eqn. 5.66 for ΔG_r, we have:

$$\Delta G_{crit} = \frac{16\pi}{3}\frac{\sigma^3 \bar{V}}{(\Delta T \Delta S_{xt})^2} \qquad (5.116)$$

If E_A is the activation energy associated with attachment of an additional atom to a cluster, then the probability of an atom having this energy is again given by the Boltzmann distribution law:

$$\mathcal{P} = e^{-E_A/\mathrm{k}T}$$

Now according to transition state theory, the frequency of attempts, ν, to overcome this energy is simply the fundamental frequency, $\nu = \mathrm{k}T/h$. The attachment frequency is then the number of atoms adjacent to the cluster, N^*, times the number of attempts times the probability of success:

$$N^* \nu \mathcal{P} = N^* \frac{\mathrm{k}T}{h} e^{-E_A/\mathrm{k}T} \qquad (5.117)$$

The nucleation rate, I, is then the attachment frequency times the number of clusters of critical radius:

$$I = N_{crit} N^* \nu \mathcal{P} = N^* \frac{\mathrm{k}T}{h} e^{-E_A/\mathrm{k}T} e^{-\Delta G_{crit}/\mathrm{k}T} \qquad (5.118)$$

Combining the frequency of attachment terms into a pre-exponential frequency factor A, and substituting 5.116 into 5.118 we have:

$$I = A e^{-16\pi\sigma^3 \bar{V}^2/(3\Delta G^2 \mathrm{k}T)} \qquad (5.119)$$

which is the usual expression for nucleation rate (e.g., McLean, 1965). If we substitute 5.66 into 5.119, we see that:

$$I = A e^{-16\pi\sigma^3 \bar{V}^2/3(\Delta S \Delta T)^2 \mathrm{k}T}$$

or

$$I \propto e^{-1/\Delta T^2} \qquad (5.120)$$

This implies that nucleation rate will be a very strong function of "temperature overstepping" for relatively small values of ΔT, but will level off at higher values of ΔT. At low degrees of overstepping, nucleation rate will be nil, but will increase rapidly once a critical temperature is achieved, as is demonstrated in Example 5.9. A more detailed treatment of nucleation and growth of crystals in cooling magmas can be found in Toramaru (1991).

Example 5.9 Nucleation of diopside

The enthalpy of fusion of diopside is 138 kJ/mol and its melting temperature is 1665 K. Assuming an activation energy of 10^{-18} J, how will the nucleation rate of diopside crystals in a diopside melt vary with temperature for surface free energies of 0.02, 0.06, and 0.12 J/m^2?

Answer: The one additional piece of information we need here is the molar volume, which we find to be 66 cc/mol from Table 2.2. We can calculate ΔS_m from the relation:

$$\Delta S_m = \frac{\Delta H_m}{T_m}$$

Assuming ΔS_m, σ, and E_A are independent of temperature, we can use eqns. 5.118 and 5.116 to calculate the nucleation rate. The calculation for the three surface free energies is shown in Figure 5.23a. Nucleation will be experimentally observable when the nucleation rate reaches $\approx 10^{-10}$ m^{-2}, which corresponds roughly to 1 nuclei/cm^2/hr. For a surface free energy of 0.02 J/m^2, the rate is reached only a few kelvins below the melting point. Further undercooling results in very high nucleation rates. For a surface energy of 0.06 J/m^2, an undercooling of 35 K is required, and an undercooling of 130 K is required at the highest value of surface energy. In the latter case, the rise in nucleation rate with undercooling is not nearly as steep.

In Figure 5.23b, we see that the nucleation rate passes through a maximum and as undercooling proceeds further, the rate decreases. This decrease reflects the 1/T dependence of both exponential terms in eqn. 5.118, i.e., the formation and growth of heterophase fluctuations will fall as temperatures falls. Observed nucleation rates show this maximum, but the "bell" is generally more symmetric and considerably narrower. This reflects the increasing viscosity of the melt, and therefore the decreasing mobility of atoms (i.e., diffusion of atoms to the proto-nuclei slows).

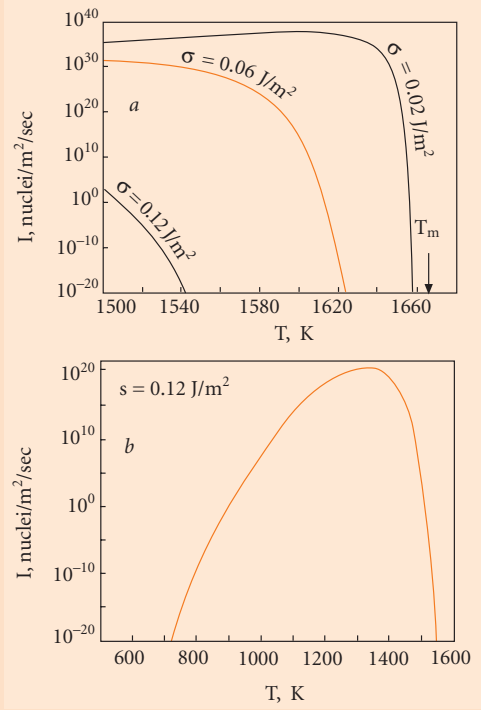

Figure 5.23 Calculated nucleation rate of diopside in diopside melt as a function of temperature.

5.5.3.3 *Heterogeneous nucleation*

The nucleation of diopside crystals from diopside melt is an example of homogenous nucleation, that is nucleation in a system where initially only one phase is present. Heterogeneous nucleation refers to the nucleation of a phase on a pre-existing one. Often the surface free energy between the nucleating phase and the pre-existing surface is lower than between the nucleating phase and the phase from which it is growing. Hence heterogeneous nucleation is often favored over homogenous nucleation. Perhaps the most familiar example is dew. Dew droplets appear on surfaces, such as those of grass, at significantly lower relative humidity than necessary for fog or mist to form. The reason is that the surface free energy between grass and water is lower than between water and air. Another example is the clusters of crystals seen in igneous rocks. These result from one crystal nucleating on the other, again because the free energy of the crystal–crystal interface is lower than that of the crystal–magma interface.

Let's examine this in a more quantitative fashion. Consider a spherical cap of phase β nucleating from phase α on a flat surface, s (Figure 5.24). The balance of surface forces at the three-phase contact is:

$$\sigma_{\alpha s} = \sigma_{\beta s} + \sigma_{\alpha\beta}\cos\theta \qquad (5.121)$$

and solving for θ

$$\cos\theta = \frac{\sigma_{\alpha s} - \sigma_{\beta s}}{\sigma_{\alpha\beta}}$$

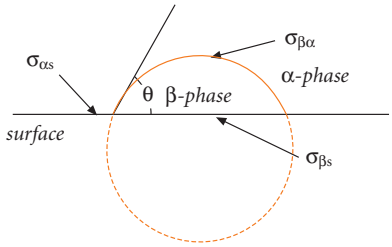

Figure 5.24 Illustration of the balance of forces as a spherical crystal or droplet of phase β crystallizes or condenses from phase α on a surface.

If the interfacial energy between the nucleating phase, β, and the surface ($\sigma_{\beta s}$) is smaller than that between phase α and the surface ($\sigma_{\beta s}$), then the angle of intersection, θ, will be small so as to maximize the interfacial surface area between β and s for a given volume of β. In the limit where $\sigma_{\beta s} \ll \sigma_{\alpha s}$ then θ will approach 0 and β will form a film coating the surface. As $\sigma_{\beta s}$ approaches $\sigma_{\alpha s}$ the nucleating phase will form more spherical droplets. If $\sigma_{\beta s} \geq \sigma_{\alpha s}$ then θ will be 90° or greater, and heterogeneous nucleation will not occur. To take account of the reduced interfacial energy between β and s, eqn. 5.115 becomes:

$$\Delta G_{crit} = \frac{16\pi}{3}\frac{\sigma_{\alpha\beta}^3 \bar{V}}{\Delta G_{xt}^2}\left(2 - 3\cos\theta + \cos^3\theta\right) \qquad (5.122)$$

In metamorphic reactions, nucleation will necessarily always be heterogeneous. Provided the necessary components of the nucleating phase are available and delivered rapidly enough by fluid transport and diffusion, interfacial energy will dictate where new phases will nucleate, nucleation being favored on phases where the interfacial energy is lowest. Where transport of components limit growth, however, this may not be the case, as phases will nucleate where the components necessary for growth are available. For example, experimental investigation of the reaction calcite + quartz ⇄ wollastonite + CO_2 revealed that, in the absence of water, wollastonite nucleated on quartz. In experiments where water was present, it nucleated on calcite. SiO_2 is not significantly soluble in CO_2, so it could not be transported in the H_2O free experiments, hence nucleation could only occur where SiO_2 was available (i.e., at the surface of quartz), despite a probable higher interfacial energy.

Unfortunately, agreement between observed and predicted nucleation rates is often poor (Kirkpatrick, 1981; Kerrick *et al.*, 1991). Equation 5.119 and Figure 5.23 show that the nucleation rate is a very strong function of the surface free energy ($I \propto \exp(\sigma^3)$), and the poor agreement between theory and observation may reflect the lack of accurate data on surface free energy as well as the activation energy, E_A. However, it may also indicate that further work on the nucleation theory is required.

5.5.3.4 *Diffusion-limited and heat-flow limited growth*

Two other kinetic factors affect crystallization. These are the local availability of energy and local availability of components necessary for crystal growth. The latter can be important where the crystal is of different composition than the liquid (almost always the case in nature, except freezing of fresh water). Crystals can grow only as rapidly as the necessary chemical components are delivered to their surfaces. Where diffusion is not rapid enough to supply these components, diffusion will limit growth.

A second effect of slow diffusion is to change the *apparent* distribution coefficient, because the crystal "sees" the concentrations in the adjacent boundary layer rather than the average concentrations in the liquid. Thus the crystal may become less depleted in elements excluded from the crystal, and less enriched in elements preferentially incorporated in it, than equilibrium thermodynamics would predict. For example, suppose a crystal of plagioclase is crystallizing from a silicate melt. Plagioclase preferentially incorporates Sr and excludes Rb. If diffusion of Sr and Rb to the crystal is slow compared with the crystal growth rate, the liquid in the boundary layer immediately adjacent to the crystal will become impoverished in Sr and enriched in Rb. The crystal will grow in equilibrium with this boundary layer liquid, not the average magma composition, thus will be poorer in Sr and richer in Rb than if it grew in equilibrium with the average magma. Figure 5.25 illustrates this point. If however, growth rate of the crystal is very much slower than the transport of components to the crystal–liquid interface, this circumstance will not arise.

When crystals grow from a magma there will be a local increase in temperature at the crystal–liquid boundary, due to release of latent heat of fusion, ΔH_m, which will retard crystal growth. In most cases, however, advection and conduction of heat is probably sufficiently rapid that this is at best a minor effect. The effect is probably more important in prograde metamorphic reactions (e.g., dehydration reactions), which are usually endothermic and hence require a continuous supply of energy to maintain crystal growth. Where crystal growth and transport of components is sufficiently rapid, heat flow may limit rates of crystal growth. This is more likely to occur at high temperatures and in late stages of metamorphism when structures are already large (Fisher, 1978).

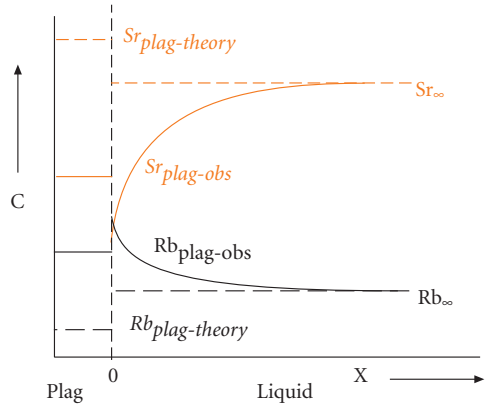

Figure 5.25 Variation of Sr and Rb concentrations from a plagioclase–liquid interface. Solid curves show the variation of concentration. The crystal–liquid interface is at 0. Dashed lines show the concentrations at infinite distance from the interface (Sr_∞, Rb_∞). Sr_{plag} and Rb_{plag} are the concentrations in the crystal.

5.5.4 Adsorption

Many geochemically important reactions take place at the interface between solid and fluid phases, and inevitably involve adsorption and desorption of species onto or from the surface of the solid. Two types of adsorption are possible: physical and chemical. Physical adsorption involves the attachment of an ion or molecule to a surface through intermolecular or van der Waals forces. Such forces are relatively weak, and heat of adsorption (ΔH_{ad}) relatively low (typically 4–12 kJ/mol). Chemical adsorption involves the formation of a new chemical bond between the adsorbed species and atoms on the surface of the solid. Heats of chemical adsorption are relatively large (>40 kJ/mol).

Adsorption of ions and molecules on a solid surface or interface affects the surface free energy. The relationship between surface

Example 5.10 The Langmuir isotherm

Consider a suspension of 1 mol/l of FeOOH. Assuming an adsorption site density of 0.1 mol/mol and K for adsorption of Sr on FeOOH of 10^5, how will the Sr adsorption density vary with the concentration of Sr in the solution? Assume that no other ions are present in the solution.

Answer: We can use eqn. 5.129 to solve this problem. Γ_M^{max} in this case is 0.1 mol/mol. Using this value and K_{ads} of 10^5 in this equation, we obtain the result shown in Figure 5.26. The inset shows that at concentrations less than about 4 μM, the adsorption density rises linearly with concentration. At higher concentrations, the adsorption density asymptotically approaches the maximum value of 0.1 mol.

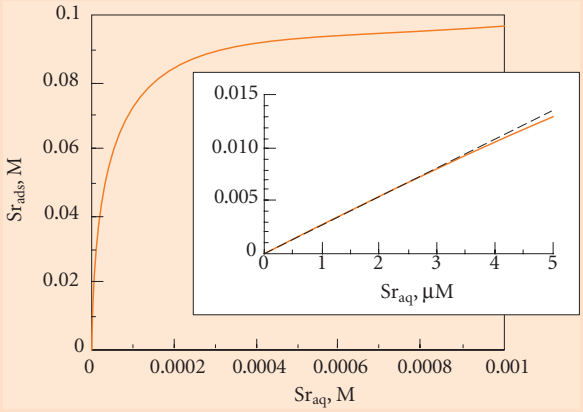

Figure 5.26 Variation of adsorption density of Sr on FeOH as a function of Sr concentration of the solution.

free energy and adsorbed ions can be expressed as:

$$d\sigma = -\sum_i \frac{n_{i,s}}{A} d\mu_i = -\sum_i \Gamma_i d\mu_i \qquad (5.123)$$

where $n_{i,s}$ is the number of mole of species i adsorbed at the surface, A is the surface area, and we define Γ_i as the *Gibbs adsorption density*. Because silicates and oxides generally have positive surface free energies, we can see that adsorption will decrease this energy and is therefore strongly favored (see Example 5.10).

5.5.4.1 The relation between concentration and adsorption: Langmuir and Freundlich isotherms

Consider the adsorption of aqueous species M at a surface site that we will denote as S. The reaction may be written as:

$$M + S \rightleftharpoons M.S$$

We will denote the fraction of surface sites occupied by M as Θ_M, the rate constant for adsorption as k_+, and that for desorption as k_-. The fraction of free sites is then $(1 - \Theta_M)$, and we explicitly assume that M is the only species adsorbed from solution. Assuming the reaction is elementary, the rate of adsorption is then:

$$\frac{dM}{dt} = k_+[M](1 - \Theta_M) \qquad (5.124)$$

The rate of desorption is:

$$\frac{d\Theta_M}{dt} = k_-\Theta_M \qquad (5.125)$$

At equilibrium, the rate of adsorption and desorption will be equal, so

$$k_-\Theta_M = k_+[M](1 - \Theta_M) \qquad (5.126)$$

Solving eqn. 5.126 for Θ_M, we obtain:

$$\Theta_M = \frac{k_+/k_-[M]}{1 + k_+/k_-[M]} \qquad (5.127)$$

which expresses the fraction of site occupied by M as a function of the concentration of M. Since at equilibrium:

$$K_{ad} = \frac{[M]_{ads}}{[M]_{aq}} = \frac{k_+}{k_-} \qquad (5.41)$$

where K_{ad} is the equilibrium constant for adsorption, eqn. 5.127 becomes:

$$\boxed{\Theta_M = \frac{K_{ad}[M]}{1 + K_{ad}[M]}} \qquad (5.128)$$

Equation 5.128 is known as the *Langmuir isotherm.** Since this is a chapter on kinetics, we have derived it using a kinetic approach, but it is a statement of thermodynamic equilibrium and can be readily derived from thermodynamics as well. From the definition of Θ_M, we may also write the Langmuir isotherm as:

$$\Gamma_M = \Gamma_M^{max} \frac{K_{ad}[M]}{1 + K_{ad}[M]} \qquad (5.129)$$

where Γ_M^{max} is the maximum observed adsorption. Thus the Langmuir isotherm predicts a maximum adsorption when all available sites are occupied by M. At large concentrations of M, then:

$$\Gamma_M = \Gamma_M^{max} \qquad (5.130)$$

Where the concentration of M is small such that $K_{ad}[M] \ll 1$, eqn. 5.128 reduces to:

$$\Theta_M \cong K_{ad}[M] \qquad (5.131)$$

This equation simply says that *the fraction of sites occupied by M is proportional to the concentration of M in solution*.

The *Freundlich isotherm,* which is purely empirical, is:

$$\boxed{\Theta_M = K_{ad}[M]^n} \qquad (5.132)$$

where n is any number. At low concentrations of M, the Langmuir isotherm reduces to the Freundlich isotherm with $n = 1$ (i.e., the amount adsorbed is a linear function of the concentration in solution).

5.5.5 Catalysis

The International Union of Pure and Applied Chemistry (IUPAC) defines *catalyst* as follows:

> *A catalyst is a substance that increases the rate without modifying the overall standard Gibbs energy change in the reaction; the process is called catalysis, and a reaction in which a catalyst in involved is known as a catalyzed reaction.*

Another definition of a catalyst is a *chemical species that appears in the rate law with a reaction order greater than its stoichiometric coefficient*. This latter definition makes it clear that a catalyst may be involved in the reaction as a reactant, a product, or neither. If it is a reactant or product, its presence affects the reaction rate to a greater extent than would be predicted from the stoichiometry of the reaction.

We can distinguish two kinds of catalysis. Homogenous catalysis refers to a situation in which the catalyst is present in the same phase in which the reaction is occurring (necessarily a solution). Examples of homogenous catalysts of geochemical reactions include acids and a collection of organic molecules called enzymes. Catalysis that occurs at the interface between two phases is referred to as heterogeneous catalysis. We will focus primarily on heterogeneous catalysis here. Heterogeneous catalysts are commonly simply surfaces of some substance. A familiar, but non-geochemical, example is the platinum in the catalytic converter of an automobile, which catalyzes the further oxidation of gasoline combustion products.

Catalysts work by providing an alternative reaction path with lower activation energy. In many cases, the lowering of the activation energy arises when reacting species are adsorbed. The heat liberated by the adsorption

* An admittedly odd name for this equation. It is named for Irving Langmuir (1881–1957). Langmuir obtained a PhD from the University of Göttingen and spent most of his career working for the General Electric Company. While trying to extend the life of light bulbs, Langmuir carried out experiments on the adsorption of gases by metals. He developed this equation to describe his results. He won the Nobel Prize for Chemistry in 1932. The term "isotherm" arises because such descriptions of adsorption are valid only for one temperature (i.e., K_{ads} is temperature-dependent, as we would expect).

(ΔH_{ads}) is available to contribute toward the activation energy. For example, consider the reaction:

$$A + B \rightarrow C$$

having an activation energy E_A. A solid catalyst of this reaction would provide the following alternate reaction mechanism:

$$A + S \rightarrow A \cdot S$$
$$B + S \rightarrow B \cdot S$$
$$B \cdot S + A \cdot S \rightarrow C \cdot S$$
$$C \cdot S \rightarrow C + S$$

The net heat of adsorption for this process is:

$$\Delta H_{ad} = \Delta H_{ad}^{A} + \Delta H_{ad}^{B} - \Delta H_{ad}^{C}$$

Recalling that enthalpy is related to activation energy, we can write the activation energy for the catalyzed reaction as:

$$E_A^{cat} = E_A + \Delta H_{ad} \qquad (5.133)$$

If ΔH_{ad} is negative (i.e., heat liberated by adsorption), the activation energy is lowered and the reaction proceeds at a faster rate than it otherwise would.

As we noted earlier, a surface will have a variety of sites for adsorption/desorption and surface reactions on a microscopic scale. Each site will have particular activation energy for each of these reactions. The activation energies for these processes will, however, be related. Sites with large negative adsorption energies also will be sites with low activation energies for surface reactions. On the other hand, if a site has a large negative adsorption energy, the desorption energy will be large and positive and desorption inhibited. If either the activation energy or the desorption energy is too large, catalysis of the overall reaction will be inhibited. What is required for fast overall reaction rates is a site where some compromise is achieved. In general, reaction and desorption energies will be related as:

$$\Delta G_r = -n\Delta G_d \qquad (5.134)$$

where n is some constant. The presence of several sites on a solid surface results in several possible reaction paths. The fastest reaction path, that is, the path that optimizes n, will dominate the reaction.

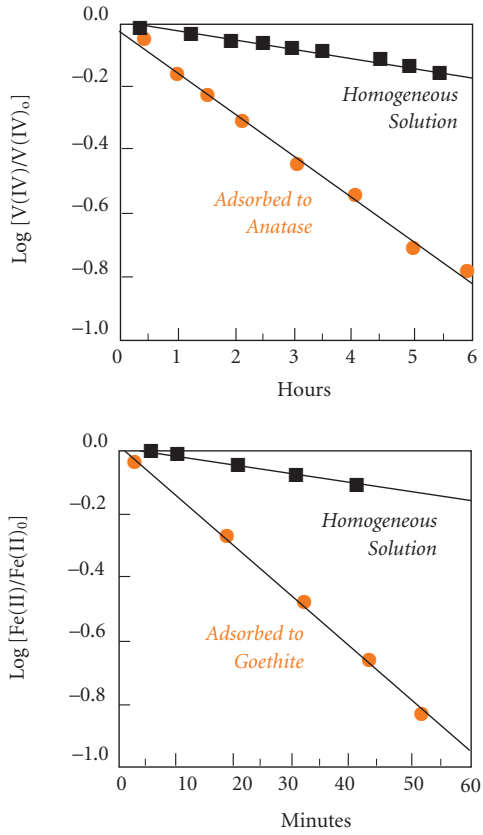

Figure 5.27 Oxygenation of vanadyl at pH 4 and $P_{O_2} = 1$ atm in experiments of Wehrli and Stumm (1988). After Wehrli *et al.* (1989). With permission from Elsevier.

Surfaces of semiconductors (metal oxides and sulfides) can catalyze oxidation–reduction reactions (e.g., Wehrli *et al.*, 1989). For example, both TiO_2 and Al_2O_3 can catalyze the oxidation of vanadyl, V(IV), to vanadate, V(V). Figure 5.27 compares the rate of reaction in the presence of TiO_2 solid to the homogenous reaction, demonstrating the reaction is substantially faster in the presence of TiO_2. The reaction mechanism for the surface catalyzed reaction may be described as follows (Figure 5.28):

$$2 >\!TiOH + VO^{2+} \rightleftharpoons >\!(TiO)_2VO + 2H^+$$
$$>\!(TiO)_2VO + TiOH \rightleftharpoons >\!(Ti)_3VO_4^{2-} + H^+$$
$$(Ti)_3VO_4^{2-} + H_2O + 2OH^- \rightleftharpoons 3 >\!TiOH + HVO_4^{2-}$$

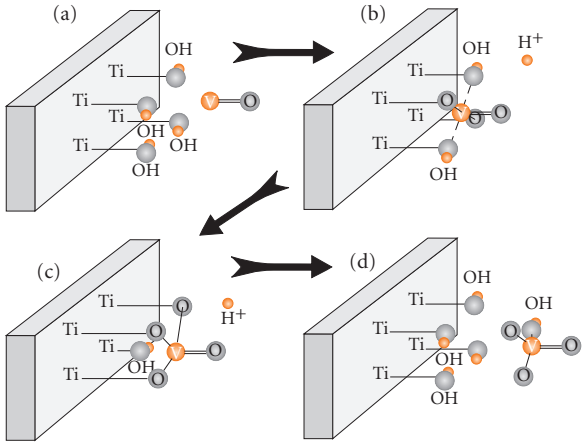

Figure 5.28 Mechanism of oxygenation of surface-bound vanadyl. In step (1) vanadyl is adsorbed at a TiO_2 surface (a → b). Note that the vanadium is bound to two surface TiO groups. In step (2), the vanadium binds to a third surface oxygen, releasing an H^+ ion (b → c). In step (3), the vanadate ion is replaced at the surface by three H^+ ions (c → d) (at intermediate pH, most vanadate will remain bound to the surface).

where >Ti indicates that the Ti atom is part of a surface. The rate law for this reaction as determined by Wehrli and Stumm (1988) is:

$$-\frac{d\{V(IV)\}}{dt} = k\{VO(OTi<)\}[O_2]$$

where the {} brackets denote surface concentrations. The reaction is thus second-order, depending on the concentration of surface bound V(IV) and dissolved O_2. Wehrli and Stumm (1988) determined the rate constant for this reaction to be $0.051\,M^{-1}s^{-1}$ and the activation energy to be 56.5 kJ/mol at pH 7.

The surface catalyzed reaction is essentially independent of pH, whereas the reaction in homogenous solution is strongly pH dependent. The rate law for the latter can be written as:

$$-\frac{d\{V(IV)\}}{dt} = k\{VO^+\}[O_2][H^+]$$

The apparent rate constant for this reaction is $1.87 \times 10^{-6}\,s^{-1}$ and the apparent activation energy is 140 kJ/mol. Part of the difference in the activation energies can be accounted for as the energy of the hydrolysis reaction:

$$VO^{2+} + H_2O \rightleftharpoons VO(OH)^+ + H^+$$

which is the first step in the homogenous reaction. This energy is 54.4 kJ/mol. Wehrli and Stumm (1988) speculated that the remainder of the difference in activation energy is the energy required for the transition from the octahedral structure of the dissolved $VO(OH)^+$ ion to the tetrahedral structure of the dissolved vanadate ion.

5.6 KINETICS OF DISSOLUTION AND LEACHING

5.6.1 Simple oxides

The rates of dissolution of non-ionic solids are generally controlled by surface reactions at the solid–water interface. Absorption of ions to the surface of the solid plays a critical role in the dissolution process. Adsorption of H^+ and OH^- ions at the surface appears to dominate dissolution reactions; however, adsorption of other species, particularly organic ones such as carboxylic acids, can be important as well.

Consider the example of a simple oxide (e.g., Al_2O_3) illustrated in Figure 5.29. As we noted earlier, "dangling" oxygens on surfaces in contact with aqueous solution will be protonated under most circumstances, that is, an H^+ ion will react with one of the surface O ligands to form a surface hydroxyl. Bonding of a single proton to a surface oxygen merely replaces the bond that the oxygen would have formed with a metal ion, had it been located in the crystal interior. Addition of a second proton (i.e., protonation of the surface hydroxyl), however, has the consequence of weakening metal-oxide bonds.

In the case of a trivalent ion such as Al_2O_3, protonation of three such bonds effectively frees the ion from the lattice structure. We can expect, therefore, that the dissolution rate will be proportional to finding three protonated ligands surrounding a single surface metal ion.

The concentration of surface-bound protons, $[H^+]_s$, can be related to the concentration of H^+ in solution through an absorption equilibrium constant K_{ad}, so that:

$$[H^+]_s/S = K_{ad}[H^+]_{aq}$$

where S is the density of surface sites. The probability of finding a metal surrounded by three protonated ligands is then proportional

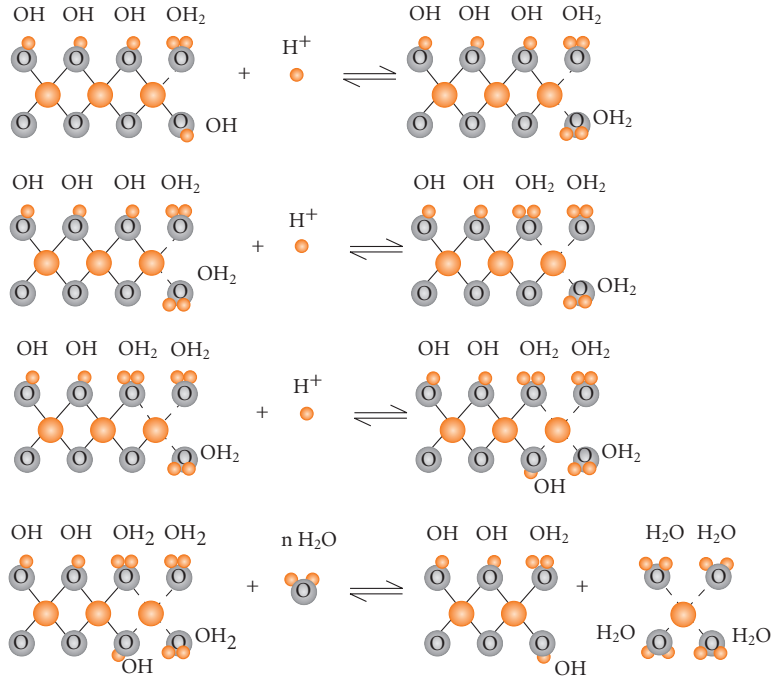

Figure 5.29 Cartoon of proton-promoted dissolution of an oxide such as Al_2O_3 at a surface step. After Stumm and Wollast (1990). With permission from John Wiley & Sons.

to $([H^+]_s/S)^3$. Thus we expect the dissolution rate to be proportional to the third power of the surface protonation:

$$\Re \propto \left\{[H_s^+]/S\right\}^3 = \left\{K_{ad}[H_{aq}^+]\right\}^3$$

Figure 5.30 shows that this is indeed the case for Al_2O_3.

Deprotonation of surface OH groups will occur at high pH through the following reaction:

$$S{-}OH + OH^- \rightleftharpoons S{-}O^- + H_2O \quad (5.135)$$

where S—O denotes a surface-bound oxygen. This deprotonation disrupts metal–oxygen bonds through polarization of electron orbitals. As a result, dissolution rates will also increase with increasing pH in alkaline solutions. Adsorption of protons at the surface is thought to be fast, hence equilibrium between adsorbed and aqueous protons is quickly attained. Thus detachment of the metal species becomes the rate-determining step. Other ligands, particularly organic ones such as

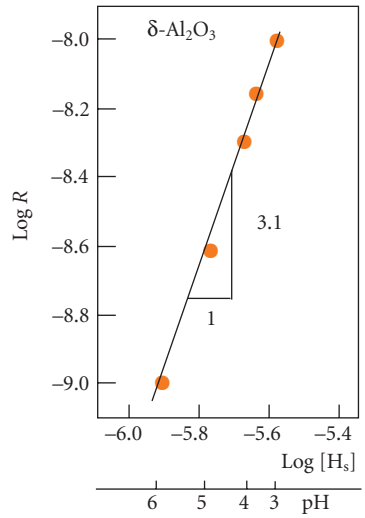

Figure 5.30 Log of the rate of Al_2O_3 dissolution plotted against the log of the concentration of surface protons. The slope of 3 indicates a rate law with third-order dependence on the surface concentration of protons. After Stumm and Wollast (1990). With permission from John Wiley & Sons.

oxalates, will have a similar effect. The overall dissolution rate is given by (Stumm and Wollast, 1990) as:

$$\Re = k_{\mathrm{H}}\left\{[\mathrm{H}_s^+]/S\right\}^i + k_{\mathrm{OH}}\left\{[\mathrm{OH}_s^-]/S\right\}^i + k_L\left\{[L_s]/S\right\}^i + k_{\mathrm{H_2O}}$$

where i is the charge on the metal ion.

5.6.2 Silicates

Surface protonation and deprotonation also play a dominant role in silicate dissolution (e.g., Blum and Lasaga, 1988). However, the dissolution of silicates is somewhat more complex than that of simple oxides because they typically contain several metals bound in different ways. This can result in incongruent dissolution, such that some metal ions may be released to solution more rapidly than others (though experiments suggest dissolution is most often congruent). A related, and particularly important, factor is lattice structure, in particular the degree to which the individual silica tetrahedra share oxygens. There is a complete range among silicates in this respect, from orthosilicates, such as olivine, in which no oxygens are shared, to the tecto-, or framework-, silicates, such as quartz and the feldspars, in which all oxygens are shared. As we discussed in Chapter 4, shared oxygens are termed bridging, and non-shared ones *non-bridging* oxygens. Sharing of oxygens increases the degree of *polymerization* of the structure.

The degree of polymerization is important in the context of dissolution because the non-bridging bonds are much more reactive than the bridging ones. Minerals with highly polymerized structures, such as feldspars, dissolve slowly and are subject to leaching, as components (particularly the network-modifiers) may be dissolved out, leaving the silicate framework still partially intact. Silicates with a low fraction of shared oxygens dissolve more rapidly and more uniformly. An example is olivine, whose structure is illustrated in Figure 5.31a. Once the Mg ions surrounding it are removed, the individual silica tetrahedra are no longer bound to the mineral, and are free to form H_4SiO_4 complexes in the solution (a more likely mode of dissolution is replacement of Mg^{2+} by $2H^+$; in essence, this produces a free H_4SiO_4 molecule). In contrast,

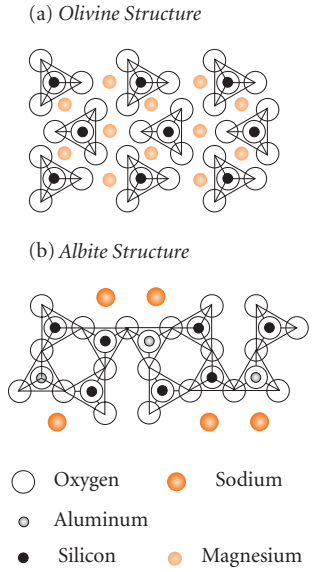

Figure 5.31 Comparison of olivine (forsterite) and feldspar (albite) structures. In feldspar, all oxygens are shared by adjacent tetrahedra, in olivine none are; instead the excess charge of the SiO_4^{4-} units is compensated by $2Mg^{2+}$.

removal of Na^+ by H^+ in albite (Figure 5.31b) leaves the framework of tetrahedra largely intact. The rate of weathering can also be affected by the Al/Si ratio, as the silicate groups are less reactive than the aluminate ones. Thus the dissolution rate of plagioclase depends on the ratio of the anorthite ($CaAl_2Si_2O_8$) to albite ($NaAlSi_3O_8$) components, with calcic plagioclase weathering more rapidly (e.g., Oxburgh *et al.*, 1994).

Some idea of the role these factors play can be obtained from Table 5.4, which lists the mean lifetimes of a 1 mm crystal for a variety of minerals in contact with a solution of pH 5 based on experimentally determined dissolution rates.

There are four important classes of reactions involved in silicate dissolution and leaching: hydration, ion exchange, leaching, and hydrolysis.

Hydration simply implies the addition of water to the structure. The effect of hydration may range from simply relaxation of the polymeric structure (e.g., swelling of vermiculite) to disruption of bridging bonds, to dissolution of polymeric fragments.

Ion exchange involves replacement of a network-modifying cation by hydrogen ions.

Table 5.4 Dissolution rates and mean lifetimes of crystals at 25°C and pH 5.

Mineral	Log rate (mol/m^2/s)	Mean lifetime years
Quartz	–13.39	34,000,000
Kaolinite	–13.28	6,000,000
Muscovite	–13.07	2,600,000
Epidote	–12.61	923,000
Microcline	–12.50	579,000
Albite	–12.26	575,000
Sanidine	–12.00	291,000
Gibbsite	–11.45	276,000
Enstatite	–10.00	10,100
Diopside	–10.15	6,800
Forsterite	–9.50	2,300
Nepheline	–8.55	211
Anorthite	–8.55	112
Wollastonite	–8.00	79

From Lasaga *et al.* (1994). With permission from Elsevier.

For example, Wollast and Chou (1992) showed that when freshly ground albite is mixed with water, there is an increase in Na^+_{aq} and an increase in pH, corresponding to the consumption of H^+_{aq}. This reaction may be represented as:

$$NaAlSi_3O_8 + H^+ \rightleftharpoons HAlSi_3O_8 + Na^+$$

This reaction, as well as the replacement of Mg^{2+} by H^+ in forsterite, has been shown to be largely reversible. Wollast and Chou (1992) found that ion exchange occurs to a depth of about 20 Å in albite, corresponding to a depth of 2 or 3 unit cells.

Leaching involves the removal of an ion without replacement by an ion from solution. The consumption of H^+ observed by Wollast and Chou (1992) was less than the production of Na^+, so that much of the Na^+ loss from the albite appears to result from leaching rather than ion exchange:

$$NaAlSi_3O_8 \rightleftharpoons AlSi_3O_8^- + Na^+$$

This reaction, of course, results in the production of negative charge on the surface. Wollast and Chou (1992) found that the extent of leaching could be related to both pH and Na^+_{aq} concentration:

$$X_{X^-} \approx 10^{-5.01} a_{H^+}^{-0.35} a_{Na^+}^{-0.65} \qquad (5.136)$$

where X_{X^-} is the mole fraction of negatively charged surface species. Thus according to eqn. 5.136, leaching increases with increasing pH and decreases with increasing aqueous Na concentration.

As we noted, structure affects the rate and degree of leaching. Sheet silicates (micas, clays, talc, serpentine) have relatively open structures though which water and solutes can be transported deeply into the structure, resulting in leaching of cations, including octahedrally coordinated Al and Mg. While the feldspar structure is not open, preferential removal of aluminate groups and charge-balance cations produces a porous structure, allowing penetration of water. Thus deep (400 Å) Na-, Ca-, and Al-poor, and Si-, H-rich layers have been observed in experimentally reacted plagioclase (Casey and Bunker, 1990).

Hydrolysis refers to the surface protonation and deprotonation reactions we have already discussed in the context of oxide dissolution. Hydrolysis has the effect of breaking of covalent metal-oxide bonds in the polymer structure by replacing them with O–H bonds. The effect is the same as replacing one of the oxygens in the tetrahedron by an OH group. Where a bridging oxygen is involved, hydrolysis decreases the degree of polymerization of the structure and eventually leads to its destruction. Complete hydrolysis of a silica tetrahedron results in the formation of a free H_4SiO_4 molecule.

This process appears to be of critical importance in the dissolution of silicates, as was the case for oxides. Many silicate dissolution experiments have shown a dependence of dissolution rate on pH of the form:

$$\Re = k a_{H^+}^n \qquad (5.137)$$

with the value of n less than one. Blum and Lasaga (1988, 1991) showed that the dissolution rate of albite can be directly related to the surface concentration of positive species ($S–OH_2^+$) under acidic conditions and to the concentration of negative surface species ($S–O^-$) under basic regions. In other words, under acidic conditions:

$$\Re = k_1[S–OH_2^+] \qquad (5.138a)$$

and under basic conditions:

$$\Re = k_2[\text{S–O}^-] \qquad (5.138b)$$

This dependence explains the fractional dependence of dissolution rate on pH. The reason is that the concentrations of S–OH_2^+ and S–O^- species can be related to pH through Freundlich isotherms (eqn. 5.132). In the case of albite dissolution, Blum and Lasaga (1991) found:

$$[\text{S} - \text{OH}_2^+] = \text{K}_1 a_{\text{H}^+}^{0.52} \qquad (5.139a)$$

$$[\text{S} - \text{O}^-] = \text{K}_2 a_{\text{OH}^-}^{0.37} = \text{K}_3 a_{\text{H}^+}^{-0.37} \qquad (5.139b)$$

for acidic and basic conditions respectively. This relationship is shown in Figure 5.32a.

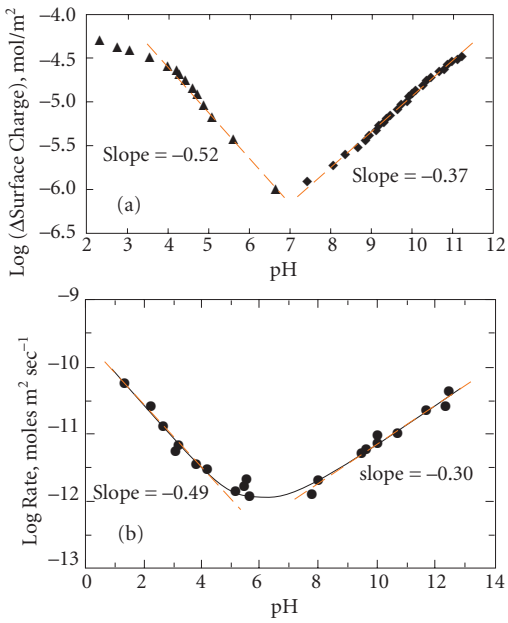

Figure 5.32 (a) Relationship between pH and the absolute value of net surface charge on dissolving albite particles. A Freundlich isotherm (dashed red lines) can be fit to the data. (b) Relationship between log of the albite dissolution rate and pH determined by Chou and Wollast (1985). The slope passing through the step parts of the curve (dashed red lines) is similar to slopes in (a), indicating that adsorption and desorption of protons controls the dissolution rate. From Blum and Lasaga (1991). With permission from Elsevier.

Substituting eqns. 5.139a and b into eqns. 5.138a and b, we expect:

$$\Re = k_3 a_{\text{H}^+}^{-0.52} \qquad (5.140a)$$

and

$$\Re = k_4 a_{\text{H}^+}^{-0.37} \qquad (5.140b)$$

This matches well the pH dependencies determined experimentally by Chou and Wollast (1985), who found the exponents in eqn. 5.136 were 0.49 and –0.30 for the acidic and basic conditions respectively, as is shown in Figure 5.32b. Although the experimental data have been questioned, a similar relationship between abundance of surface species and dissolution rate has been claimed for olivine.

Ganor *et al.* (1995) demonstrated that the dissolution rate of kaolinite ($\text{Al}_2\text{Si}_2\text{O}_5[\text{OH}]_4$) also shows a fractional exponential dependence on pH (eqn. 5.138), with the value of the exponent, n, being 0.4 ± 0.2 for the pH range 3 to 4. Consistent with earlier studies, they concluded that the form of the rate equation reflected the equilibrium adsorption of protons on the mineral surface. Their interpretation of the details of the reaction mechanism, however, was somewhat different from the interpretation of the mechanism of Al_2O_3 dissolution of Stumm and Wollast (1990) discussed above. Ganor *et al.* (1995) argued that simultaneous protonation of all metal-oxide bonds was unlikely and furthermore unnecessary, since stepwise breaking of metal-oxide bonds would do the job. They argued that hydrogen ion–mediated breaking of Al–O–Si bonds was the critical and rate-determining step in kaolinite dissolution. In support of this hypothesis, they pointed out that *ab initio* (i.e., from first principles) calculations show that the activation energy for hydrolysis of this bond is lower than that of Si–O–Si bonds. The kaolinite structure (Figure 5.33) consists of alternating sheets of Si-tetrahedra and Al-octahedra, with each Si-tetrahedron sharing an oxygen with an Al in the octahedral layer. Breaking these Al–O–Si bonds effectively "unzips" the octahedral and tetrahedral sheets. Subsequent hydrolysis of the individual metal–oxygen bonds is then fast.

In focusing on the effects of pH in our discussion of dissolution thus far, we have implicitly assumed that dissolution reactions

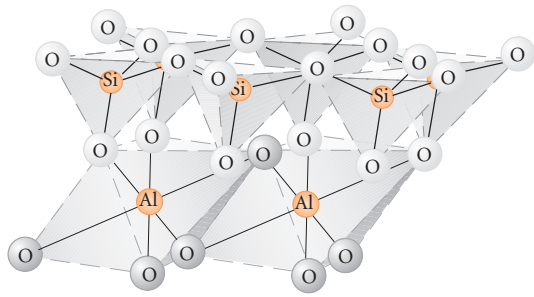

Figure 5.33 The structure of kaolinite. Kaolinite consists of a layer of Si-tetrahedra linked to a layer of Al-octahedra through a shared oxygen.

take place far from equilibrium. We have also ignored the effects of temperature. Clearly, temperature and the approach to equilibrium must be taken into account in a full treatment of dissolution. Furthermore, other dissolved species might either catalyze or inhibit dissolution reactions. Lasaga *et al.* (1994) proposed the following rate equation to take account of these additional factors:

$$\Re = k_0 e^{-E_A/RT} f(\Delta G) A_{\min} a_{H^+}^n \prod_i a_i^{m_i} \qquad (5.141)$$

The $k_0 e^{-E_A/RT}$ term is the usual Arrhenius expression for temperature dependence. A_{min} is the surface area of the dissolving mineral, the term $a_{H^+}^n$ takes account of the pH dependence, and the $a_i^{m_i}$ terms take account of the inhibitory or catalytic effects of other ions; n and m_i may take any value. The $f(\Delta G)$ term is some function of ΔG that expresses the dependence of the rate on the deviation from equilibrium. For instance, we saw that transition state theory predicts that $f(\Delta G)$ for an elementary reaction takes the form of eqn. 5.57, i.e.:

$$f(\Delta G) = k(1 - e^{-\Delta G/RT})$$

For an overall reaction, $f(\Delta G)$ might have the form (eqn. 5.58):

$$f(\Delta G) = k(1 - e^{-n\Delta G/RT})$$

Even if the exact form of the rate equation is not known, an apparent activation energy can be calculated to express the temperature dependence of reaction rate. In that case, however, the activation energy is valid only under a specific set of conditions. Values of such apparent activation energies for a few minerals are listed in Table 5.5.

Table 5.5 Apparent activation energies for dissolution reactions.

Mineral	E_a kJ/mol	pH
Albite	54.4	Neutral
Albite	32.2	Basic
Albite	117.2	<3
Epidote	82.9	1.4
Kaolinite	29.3	3–4
Microcline	52.3	3
Quartz	71.2	7
Sanidine	54.0	3
Wollastonite	79.1	3-8

Modified from Lasaga *et al.* (1994). With permission from Elsevier.

Equation 5.141 predicts that the dissolution rate will slow as equilibrium between mineral and solution is approached (i.e., as the concentration of dissolved components increases). This will occur when the rate of dissolution exceeds the rate of transport because the concentrations of dissolution products will build up at the mineral–water interface. In the steady state, mass balance requires that the rate of dissolution (i.e., the rate at which aqueous species are produced at the surface) and transport (the rate at which components are removed from the solution adjacent the dissolving surface) must be equal. Thus overall weathering rates are controlled by a combination of surface kinetics and transport kinetics. In each individual situation, one or the other can be the rate-limiting step.

Surface reactions are most often rate-limiting in dissolution and weathering of silicate minerals at low temperature (25°C). Dissolution of readily soluble minerals (e.g., halite) and even moderately soluble minerals (e.g., gypsum) are, by contrast, usually limited by the rate at which the dissolving components can be transported away from the mineral–water interface by advection and diffusion. As temperature increases, transport is increasingly likely to become rate-limiting. This is because the activation energy of diffusion in aqueous solution, typically 5–10 kJ/mol, is

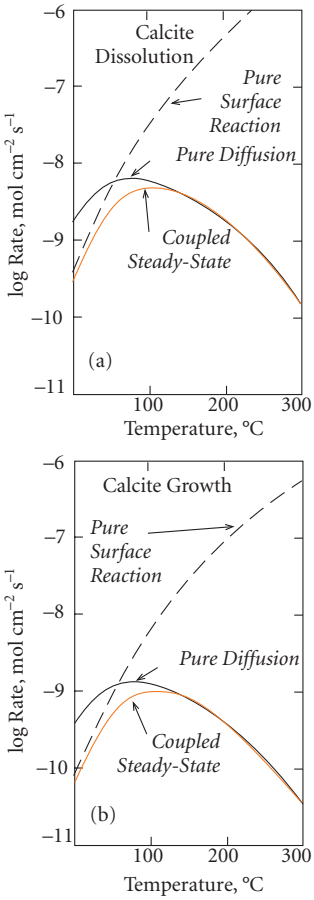

Figure 5.34 Log of steady-state dissolution (a) and growth (b) of calcite as a function of temperature, comparing diffusion-controlled and surface reaction-controlled kinetics. The model assumes a 1 μm hydrodynamic boundary layer and saturation in the case of growth. From Murphy *et al.* (1989). With permission from Elsevier.

generally less than the activation energy of surface reactions (typically >30 kJ/mol; Table 5.5). Thus the diffusion rates increase more slowly with temperature than surface reaction rates. This point is illustrated for the case of calcite in Figure 5.34. At temperatures below 75°C, growth and dissolution of calcite, a moderately soluble mineral, is effectively controlled by the surface reaction rate, while at temperatures greater than 125°C, diffusion is the rate-controlling step. Dissolution under hydrothermal and metamorphic conditions is most likely to be diffusion-controlled for most minerals (Guy and Schott, 1989).

5.7 DIAGENESIS

An introductory geology text might define *diagenesis* as the process through which sediment is converted to a sedimentary rock. We will use diagenesis to refer to a number of physical and chemical processes that occur subsequent to deposition of sediment, including compaction and expulsion of pore water, consumption of organic matter, and resulting changes in $p\varepsilon$. Some of the originally deposited phases dissolve in the pore water during diagenesis; other phases crystallize from the pore water. Some of these changes begin immediately after deposition, some only as a result of later deformation. Some occur as a result of moderately elevated temperature and pressure, though processes occurring at significantly higher temperature and pressure would be called metamorphism. Diagenesis and metamorphism form a continuum; though a geologist might volunteer a definite opinion on whether a particular specimen had been diagenetically or metamorphically altered, he would be hard pressed to come up with criteria to distinguish diagenesis from metamorphism that were not arbitrary. Here, we will briefly consider a few of these processes.

5.7.1 Compositional gradients in accumulating sediment

Let's turn our attention to the early stages of diagenesis in slowly accumulating sediment. Our first task is to decide upon a reference frame. There are two choices: we could choose a reference frame fixed to a specific layer. In this case, the sediment–water interface will appear to move upward with time. Alternatively, we can choose a reference frame that is fixed relative to the sediment–water interface, thus depth always refers to distance downward from that interface. As sediment accumulates, a given layer of sediment will appear to move downward in this reference frame. In this reference frame, we can express the change in concentration at some depth, x, as the sum of changes in the composition due to diagenesis plus the change in the composition of sediment flowing downward past our fixed reference point:

$$\left(\frac{\partial C}{\partial t}\right)_x = \frac{dC_i}{dt} - \omega\left(\frac{\partial C_i}{\partial x}\right)_t \qquad (5.142)$$

where C_i is concentration of some species i, and ω is the burial rate. The partial derivative on the left-hand side refers to changes *at some fixed depth*, and the total derivative refers to diagenetic changes occurring in a given layer, or horizon, undergoing burial. $(\partial C_i/\partial x)_t$ is the concentration gradient of i at some fixed time t. This equation allows us to convert a reference frame that is fixed relative to the sediment–water interface to one that is fixed relative to some sedimentary layer.

Now let's consider two extremes where eqn. 5.142 is particularly simple. In the first, a steady state is reached and there is no change with time, hence:

$$\left(\frac{\partial C}{\partial t}\right)_x = 0 \qquad (5.143)$$

In other words, the concentration of i at some fixed depth below the water–sediment interface is constant. Under these circumstances then,

$$\frac{dC_i}{dt} = \omega\left(\frac{\partial C_i}{\partial x}\right)_t \qquad (5.144)$$

This case is illustrated in Figure 5.35.

In the second extreme, there is no diagenesis and the composition of a given layer is determined only by what is initially deposited, thus:

$$\frac{dC_i}{dt} = 0 \qquad (5.145)$$

The concentration change with time at some fixed depth is then due to change in the composition of the sediment moving downward past that point. Thus:

$$\left(\frac{\partial C_i}{\partial t}\right)_x = \omega\left(\frac{\partial C_i}{\partial x}\right)_t \qquad (5.146)$$

This case is illustrated in Figure 5.36.

The sediment consists both of solid particles and the water buried with the particles, the pore water. Assuming no other fluid is present (e.g., gas, petroleum) then the volume fraction of water in the sediment is equal to the porosity ϕ. The volume fraction of solids is then simply $1 - \phi$. Most sediments will undergo compaction as they are buried. This is due to the weight of overlying sediment (gravitational compaction). Gravitational compaction results in expulsion of pore water and a decrease in porosity with depth. In addition, dissolution and cementation will also affect porosity. Since the molar volume of a phase precipitating or dissolving (the most impor-

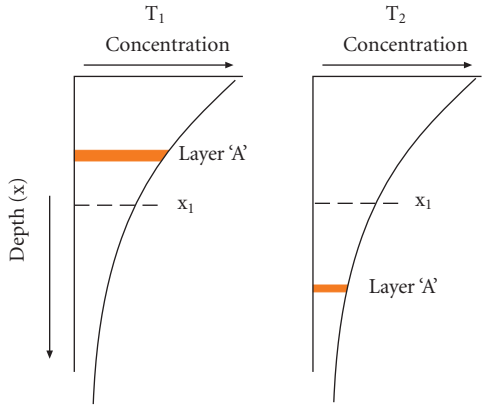

Figure 5.35 Steady-state diagenesis. Concentration at a fixed depth x_1 below the surface remains constant, but layer A, whose depth increases with time due to burial, experiences a decreasing concentration with time. After Berner, Robert A: Early Diagenesis © 1980 Princeton University Press. Reprinted with permission of Princeton University Press.

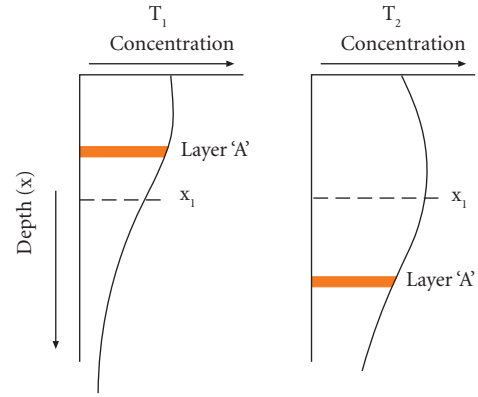

Figure 5.36 Concentration profiles in a sediment in which the composition of the material changes with time, but there is no diagenesis. The composition of any given layer is fixed, but the composition at some fixed depth relative to the water–sediment interface, such as x_1, changes with time. After Berner, Robert A: Early Diagenesis © 1980 Princeton University Press. Reprinted with permission of Princeton University Press.

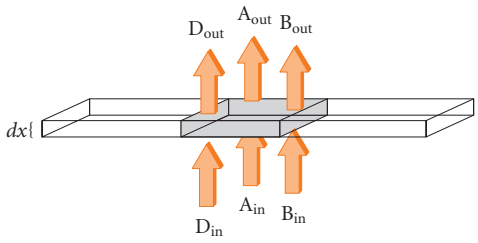

Figure 5.37 Fluxes through a box in a sedimentary layer of unit lateral dimensions and thickness *dx*. Arrows labeled A, B, and D indicate advective, biodiffusive, and molecular diffusive fluxes, respectively. Loss or gain by the box due to these processes depends on the difference in the flux into and out of the box: *dF/dx*.

tant such phase is often $CaCO_3$) will be different from its partial molar volume in solution, these processes will also result in motion of the pore water. When compaction occurs, the rate of burial of sediment will not be equal to the sedimentation rate.

Now consider a box of sediment of thickness *dx* and unit length and width embedded within some sedimentary layer (Figure 5.37). We assume that the layer is of uniform composition in the lateral dimension, and therefore that there is no lateral diffusion, and that there is also no lateral advection of fluid. Within the box there are *C* moles of species *i*. If we chose our concentration units to be moles per volume, then the concentration is simply C_i.

Let's consider the processes that can affect the concentration of species *i* within the box. First of all, reactions occurring within the box might affect *i*. For example, oxidation and reduction will affect species such as Fe^{3+}, SO_4^{2-}, and Mn^{2+}. If we are interested in the concentration of a dissolved species, then dissolution, crystallization, leaching, and so on, will all change this concentration.

In addition to reactions occurring within the box, diffusion, advection, and bioturbation will also affect the concentration of *i* if there is a difference between the fluxes into and out of the box. Bioturbation is the stirring effect produced by the activity of animals that live in the sediment (the infauna). From a geochemical perspective, bioturbation is much like diffusion in that it results from the random motion of particles (even if these particles are of very different size from atoms and ions) and acts to reduce compositional gradients. Mathematically, we can treat the effect of bioturbation in a way similar to diffusion, that is, we can define a bioturbation flux as:

$$J_B = -D_B\left(\frac{\partial C_i}{\partial x}\right)_t \qquad (5.147)$$

where D_B is the biodiffusion coefficient. Values of D_B for solid phases range from 10^{-6} cm^2/sec in nearshore clays to 10^{-11} in deep-sea pelagic sediments. The bioturbation coefficient will generally be different for solid species than for liquid ones. Since most animals live in the upper few centimeters of sediment, D_B will be a function of depth. In those circumstances, the time dependence of concentration is given by:

$$\left(\frac{\partial C}{\partial t}\right)_x = \left\{\frac{\partial(D_B(\partial C_i / \partial x))}{\partial x}\right\}_t \qquad (5.148)$$

Since molecular diffusion through solids is much lower than through liquids, one can generally neglect diffusion in the solid and deal only with diffusion through the pore water. Because pore water only occupies a fraction, ϕ, of the total volume of sediment, the flux will be reduced accordingly. Thus the diffusion of a dissolved species will be:

$$J_M = -\phi D_M\left(\frac{\partial C_i}{\partial x}\right) \qquad (5.149)$$

where we have adopted the subscript M to denote molecular diffusion. Fick's Second Law becomes:

$$\left(\frac{\partial C_i}{\partial t}\right)_x = \frac{1}{\phi}\frac{\partial(\partial\phi D_M(\partial C_i / \partial x))}{\partial x} \qquad (5.150)$$

The advective flux is the product of the fluid (i.e., pore water) velocity times the concentration:

$$J_A = vC_i \qquad (5.151)$$

To describe the rate of change of concentration in the box, we want to know the rate of reactions within it and the change in flux across it, as it is the change in flux that dictates what is lost or gained by the box. Combining all the fluxes into a single term, F_i, the rate of change of species *i* in the box is:

$$\frac{dC_i}{dt} = -\frac{\partial F_i}{\partial x} + \sum R_i \qquad (5.152)$$

where the second term is the sum of the rates of all reactions affecting *i*. The flux term is negative because any decrease in flux over *dx* results in an increase in concentration within the box.

We can then use equation 5.142 to transform to a reference frame fixed relative to the sediment surface:

$$\left(\frac{\partial C_i}{\partial t}\right)_x = -\left(\frac{\partial F_i}{\partial x}\right)_t - \omega\frac{\partial C_i}{\partial x} + \sum R_i \qquad (5.153)$$

The downward burial of sediment past point *x* can also be considered a flux. Combining this with the other flux terms, we have:

$$\boxed{\left(\frac{\partial C_i}{\partial t}\right)_x = -\left(\frac{\partial F_i}{\partial x}\right)_t + \sum R_i} \qquad (5.154)$$

where *F* is the *net* flux of *i* in and out of the box and the last term is the rate of all internal changes, including chemical, biochemical, and radioactive, occurring within the box. Equation 5.154 is called the *diagenetic equation* (Berner, 1980). Let us now consider an example that demonstrates how this equation can be applied.

5.7.2 Reduction of sulfate in accumulating sediment

Organic matter buried with the sediment will be attacked by aerobic bacteria until all dissolved O_2 is consumed. When O_2 is exhausted, often within tens of centimeters of the surface, consumption will continue anaerobically, with sulfur in sulfate acting as the electron acceptor:

$$2\alpha CH_2O + SO_4^{2-} \rightarrow H_2S + 2HCO_3^- \qquad (5.155)$$

where CH_2O represents organic matter generally and α is the number of organic matter carbon atoms reduced per sulfur atom. Let's assume that the rate of sulfate reduction depends only on the supply of organic matter and not on the abundance of sulfate. In this case:

$$\frac{d[CH_2O]}{dt} = -k[CH_2O] \qquad (5.156)$$

We are greatly simplifying matters since there are a great variety of organic compounds in sediments, each of which will have a different rate constant. To further simplify matters, we will assume (1) that conditions become anaerobic at the sediment–water interface, (2) that all consumption of organic matter occurs anaerobically, (3) that steady-state is achieved (i.e., $(\partial C/\partial t)_x = 0$), and (4) there is no compaction (and therefore no pore water advection) or bioturbation. Substituting 5.156 into 5.146, we have:

$$-k[CH_2O] = \omega\left(\frac{\partial[CH_2O]}{\partial x}\right)_t \qquad (5.157)$$

Integrating, we obtain the concentration of organic matter as a function of depth:

$$[CH_2O](x) = [CH_2O]^\circ e^{-kx/\omega} \qquad (5.158)$$

where $[CH_2O]^\circ$ is the organic matter concentration at the sediment–water interface (x = 0).

We can now also solve for the variation in concentration sulfate in the pore water. According to eqn. 5.7, the rate of sulfate reduction is related to the organic matter consumption rate as:

$$\frac{d[SO_4^{2-}]}{dt} = \frac{1}{2\alpha}\frac{d[CH_2O]}{dt} = \frac{k[CH_2O]^\circ}{2\alpha}e^{-kx/\omega} \qquad (5.159)$$

Whereas the organic matter can be considered fixed in sediment, the sulfate is a dissolved species, so we must also consider diffusion. Making appropriate substitutions into 5.154, we have:

$$\phi D\left(\frac{\partial^2[SO_4^{2-}]}{\partial x^2}\right) - \omega\left(\frac{\partial[SO_4^{2-}]}{\partial x}\right)_t - \frac{k[CH_2O]^\circ}{2\alpha}e^{-kx/\omega} = 0 \qquad (5.160)$$

This is a second-order differential equation and its solution will depend on the boundary conditions. Our boundary condition is that at x = 0, C = C°. The solution under these conditions is:

$$[SO_4^{2-}] = \frac{\omega^2[CH_2O]^\circ}{2\alpha(\omega^2 + kD)\phi}\left(e^{kx/\omega} - 1\right) + [SO_4^{2-}]^\circ \qquad (5.161)$$